Works on CO data

- Download the CO data observed by Delingha 13.7m telescope, it is a large file: *co_data.14m*
- Learn GILDAS/CLASS software to read & analyse the above CO data, tutorials can be found in /co12/ref/.

1. Aim:

- Estimate the Molecular Column Density N_{H2} towards each Millennium Survey sightlines by using the X-Factor X_{CO}:

$$N_{H2} = 2X_{CO}W_{CO}$$

$$N^{total}_{H} = N_{HI} + N_{H2} = N_{HI} + 2X_{CO}W_{CO}$$

- Use dust conversion factor σ_{353} from Planck papers on CO and thermal dust emission at 353GHz, to calculate the *Total Proton Column Density* N_H from in the direction of Millennium Survey sightlines.

$$\tau_{353} = \sigma_{353} * N_H.$$

Note: in the paper, σ_{353} varies with Galactic *l,b*

→ To see if the differences between the estimates made by (optically thin N(H) + CO-based H_2) Column Densities and dust-based Column Densities can be explained ONLY by HI opacity effects, OR we need other components.

---

2. GILDAS software

- CO data from Delingha 13.7m telescope have been observed and taken in format of GILDAS optimised for Single-dish analysis.
- I installed GILDAS software and its interactive program CLASS *(Continuum and Line Analysis Single-dish Software)* which is dedicated to the processing of single-dish spectra.
- Delingha antenna Performance
  - *Enclosed in a High-Transparency Radome (85-90%)*
  - *Diameter: 13.7 m*
  - *Pointing Accuracy: < 10" over the whole sky*
  - *Beamwidth (HPBW): ~60"*
  - *Aperture Efficiency: 39%*
  - *Main Beam Efficiency: 77%*
  - *Surface Accuracy: ~0.1 mm*
- Delingha 13.7 m radio telescope equipped with a 3x3 pixel multi-beam side-band separation receiver. There are 9 beams in total and each beam has two side-bands which are upper side band and lower side band.
- When mapping, all the 9 beams are used. When observing only one positions, they use all the beams but only one beam is pointed to the source.
- For instance, B3LS means beam 3, lower side band, B6US means beam 6 upper side band.
- Notice that the 3x3 array in the telescope cannot rotate. Consequently, when observing only one position, the data from the beam, which is pointed to the source, is the only usable one.
- In total, 101 sources were observed using 3 lines: 12CO(1-0), 13CO(1-0) and C18O(1-0) and 9 beams: B3LS, B5LS, B6LS, B8LS, B3US, B5US, B6US, B8US, B9US...
- Unfortunately, 27 MS sources (Heiles 2003) have NOT been observed: 3C79, CTA21, P0320+05, NRAO140, 3C93.1, P0347, 3C172.0, DW0742+10, 3C190.0, P0820+22, 3C208.0, 3C208.1, 3C223, 3C228.0, 3C234, 3C236, P1117+14 3C263.1, 3C264.0, 3C267.0, 3C272.1, 4C07.32,

4C32.44, 3C286, 3C293, 4C19.44, 4C20.33
- For each source, 60 observations have been taken: 20 for 13CO(1-0), 20 for C18O(1-0) and 20 for 12CO(1-0) with different offsets (Figure 1).

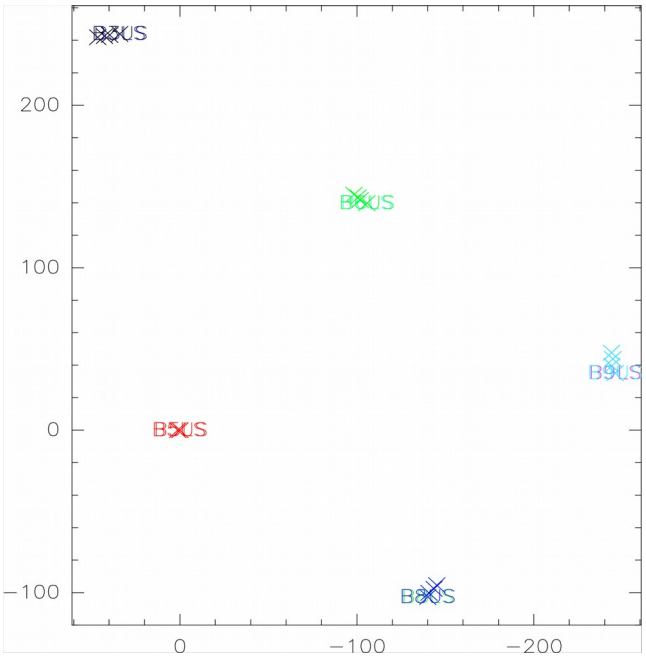

Figure 1: 60 observations of 3C123 as a typical example using 3 CO lines at different offsets, units are arcseconds.

- 18 sources with presence of ^{12}CO (1-0) peaks have been found, they are: 3C105, 3C123, 3C131, 3C133, 3C154, 3C167, 3C207, 3C353, 3C410, 3C454.3, 3C75, 4C13.67, 4C22.12, G196.6+0.2, G197.0+1.1, P0428+20, T0526+24, T0629+10.

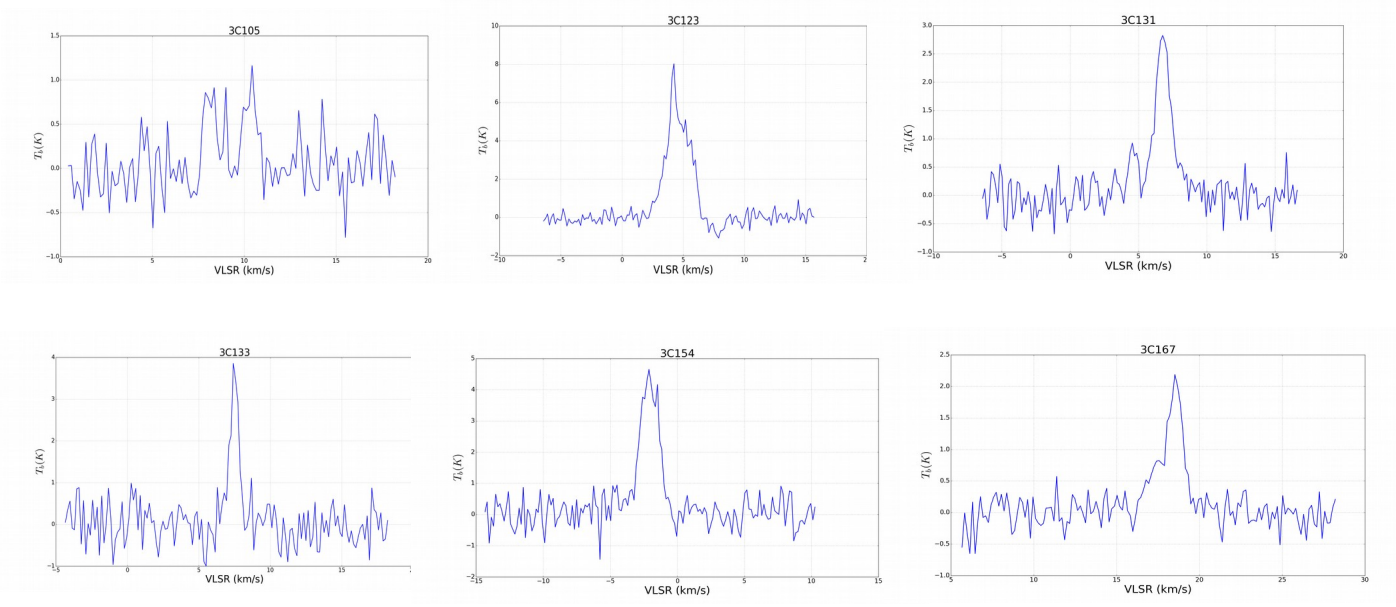

Figure ??: Typical examples of ^{12}CO(1-0) spectra.

- I then calculated *the velocity integrated main beam brightness temperature*, W_{CO}, in K km/sec, the

W_{CO} values obtained are comparable/same order with the W_{CO} values from Dame et al. 2001, see the table below for more details:

#	src	beam	l	b	xplane	yplane	v1	v2	vx1	vx2	wco	wco_dame	%
0	3c105f.dat	b5us	187.6	-33.6	-	-	7.38	11.05	-	-	1.57	-	-
1	3c123f.dat	b5us	170.6	-11.7	75	147	1.98	6.4	245	255	14.25	12.13	-14.87%
2	3c131f.dat	b5us	171.4	-7.8	69	178	3.83	8.65	245	260	4.87	3.01	-38.19%
3	3c133f.dat	b5us	177.7	-9.9	18	161	5.65	8.84	248	254	3.05	5.13	+68.19%
4	3c154f.dat	b2us	185.6	4.0	0	273	-5.67	0.07	240	253	8.27	2.77	-66.51%
5	3c167f.dat	b2us	207.3	1.2	-	-	15.57	20.25	-	-	3.25	-	-
6	3c207f.dat	b2us	213.0	30.1	-	-	3.63	7.16	-	-	0.45	-	-
7	3c353f.dat	b5us	21.1	19.9	-	-	-2.3	1.17	-	-	4.08	-	-
8	3c410f.dat	b5us	69.2	-3.8	886	210	4.86	7.06	245	263	1.44	1.74	+20.83%
9	3c4543f.dat	b5us	86.0	-38.1	-	-	-10.67	-7.27	-	-	4.31	-	-
10	3c75f.dat	b5us	170.3	-44.9	-	-	-11.56	-9.03	-	-	1.55	-	-
11	4c1367f.dat	b2us	43.5	9.2	1092	313	2.33	9.02	245	255	14.26	8.97	-37.10%
12	4c2212f.dat	b2us	188.1	0.0	-	-	-4.11	-1.17	-	-	2.33	-	-
13	g196602f.dat	b2us	196.6	0.2	-	-	0.98	5.05	-	-	0.69	-	-
14	g197011f.dat	b2us	197.0	1.1	-	-	1.05	9.28	-	-	6.62	-	-
15	p042820f.dat	b5us	176.8	-18.6	-	-	9.41	12.03	-	-	1.13	-	-
16	t052624f.dat	b2us	181.4	-5.2	0	199	4.25	9.81	245	257	10.3	4.31	
17	t062910f.dat	b2us	201.5	0.5	-	-	-0.84	8.5	-	-	43.12	-	-58.16%

Table ??: The velocity integrated main beam brightness temperature of $^{12}CO(1\text{-}0)$, W_{CO}.

- In total, there are 42 common sources between Delingha observation and MS survey. Hence, there are 26 sources without the presence of CO, it means traditionally there would not be H_2 along the line-of-sight, now I will look at these sources in details.
- From Ningyu's results, he also found the same 26 lines-of-sight without CO, and the same 18 lines-of-sight where CO is present.

3. Thermal dust emission τ_{353} to total proton column density N_H

- The Planck paper on All-sky model of thermal dust emission (2013) (https://arxiv.org/pdf/1312.) indicates a link between the optical depth of thermal dust emission at 353GHz, τ_{353}, and the total gas column density N_H:

$\tau_{353} = \sigma_{353} * N_H$ *(1)*

where: σ_{353}*:* dust-to-gas conversion factor

τ_{353} map and τ_{353} error map (release R1.20) can be accessed here:
http://irsa.ipac.caltech.edu/data/Planck/release_1/all-sky-maps/previews/HFI_CompMap_ThermalDustModel_2048_R1.20/index.html

- Note that the values of σ_{353} vary from region to region as shown in Table 3.

Mask	$<\sigma_{353}>$ [cm^2H^{-1}]	$\sigma(\sigma_{353})$ [cm^2H^{-1}]
Whole sky	$8.4x10^{-27}$	$3.0x10^{-27}$
G56	$7.1x10^{-27}$	$1.9x10^{-27}$
$\|b\| > 15^o$	$7.0x10^{-27}$	$2.0x10^{-27}$
G45	$6.8x10^{-27}$	$1.8x10^{-27}$
G35	$6.5x10^{-27}$	$1.8x10^{-27}$
South Cap	$6.5x10^{-27}$	$1.9x10^{-27}$
Low N_{HI}	$6.6x10^{-27}$	$1.7x10^{-27}$
Lowest 1%	$7.9x10^{-27}$	$1.9x10^{-27}$

Table ??: Mask used in Planck 2013 paper for the values of $<\sigma_{353}>$ and its uncertainties $\sigma(\sigma_{353})$.

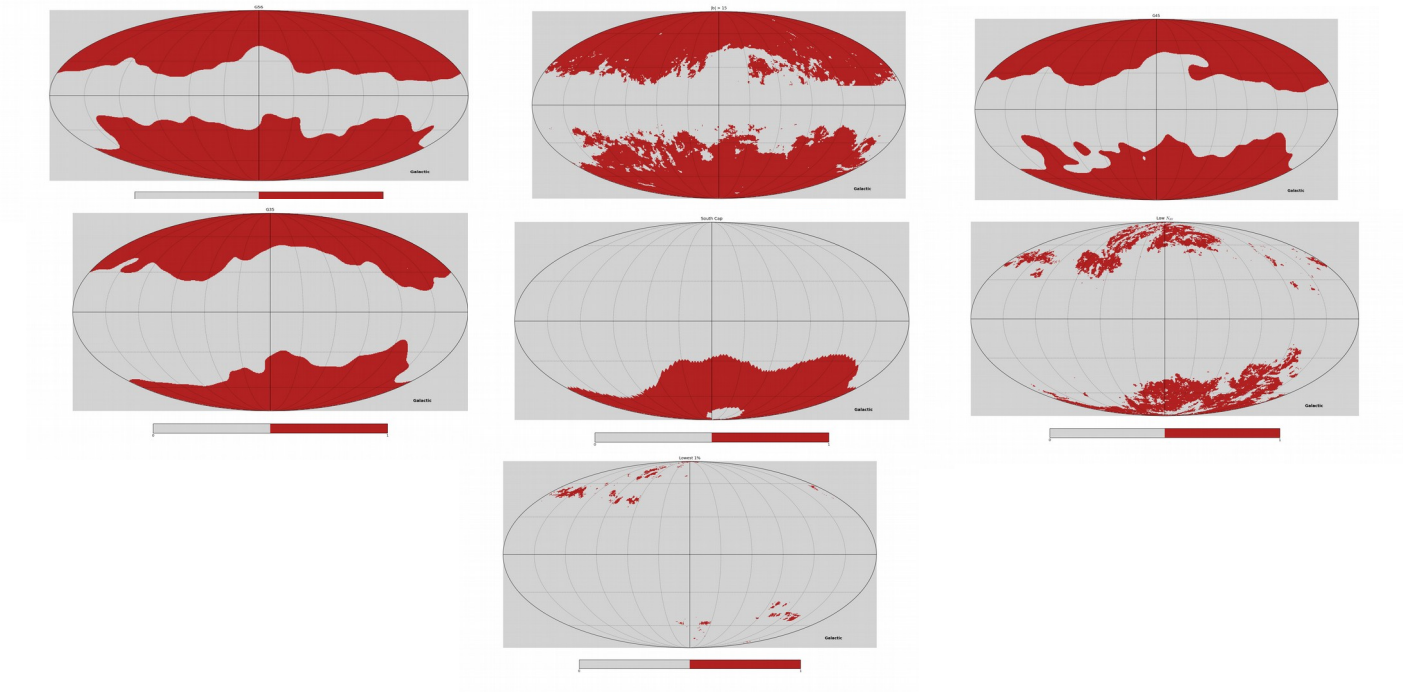

Figure ??: The masks from Planck 2013 paper.

- I use the equation (1) to calculate the total gas column densities N_H along 26 lines-of-sight where CO lines are not detected.
- I installed HEALPix software (in Python, it is healpy package) to read Planck FITS data file, the optical depth map of thermal dust emission at 353GHz, τ_{353}, in Mollview, and Cartview is displayed in Figure ??:

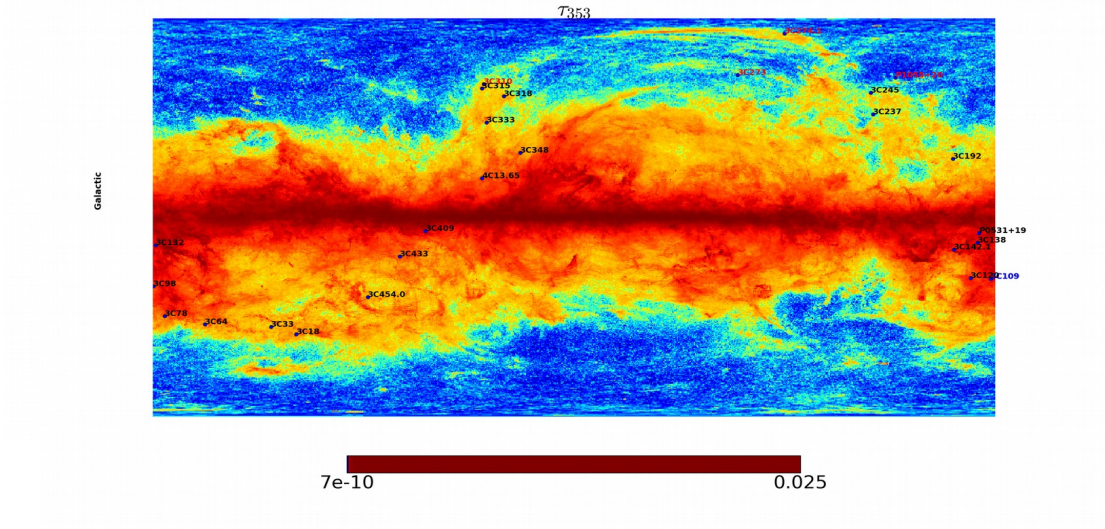

Figure ??: Optical depth map of thermal dust emission at 353GHz, τ_{353}, in Mollview and Cartview and positions of 26 sources without CO.

- I also calculate the Total Proton Column Density N_H from τ_{353} for the above 26 MS line-of-sights using Fukui conversion factors (Fukui et al. 2015), namely:

$N_H = [2.0 \times 10^{26} \pm <\text{no error}>] * \tau_{353}$ *(2)*

The purpose of this is to compare and check if there exists a consistency (?^^?).

- For selected MS line-of-sights, I compute the Mean Value of τ_{353} in an area about the Arecibo Beam (3.5').
- It means:
  - Define a very small area around the point-source at (l_0,b_0) with the radius of 3.5 arcmin, the beam of Arecibo telescope.
  - Find the pixels within the area.
  - Get the value of optical depth τ_{353} in each pixel.
  - Take the average of all τ_{353} values, and this is the value of τ_{353} obtained.

- The τ_{353} error for each point source will similarly be calculated.

- Examples are shown in figure ??

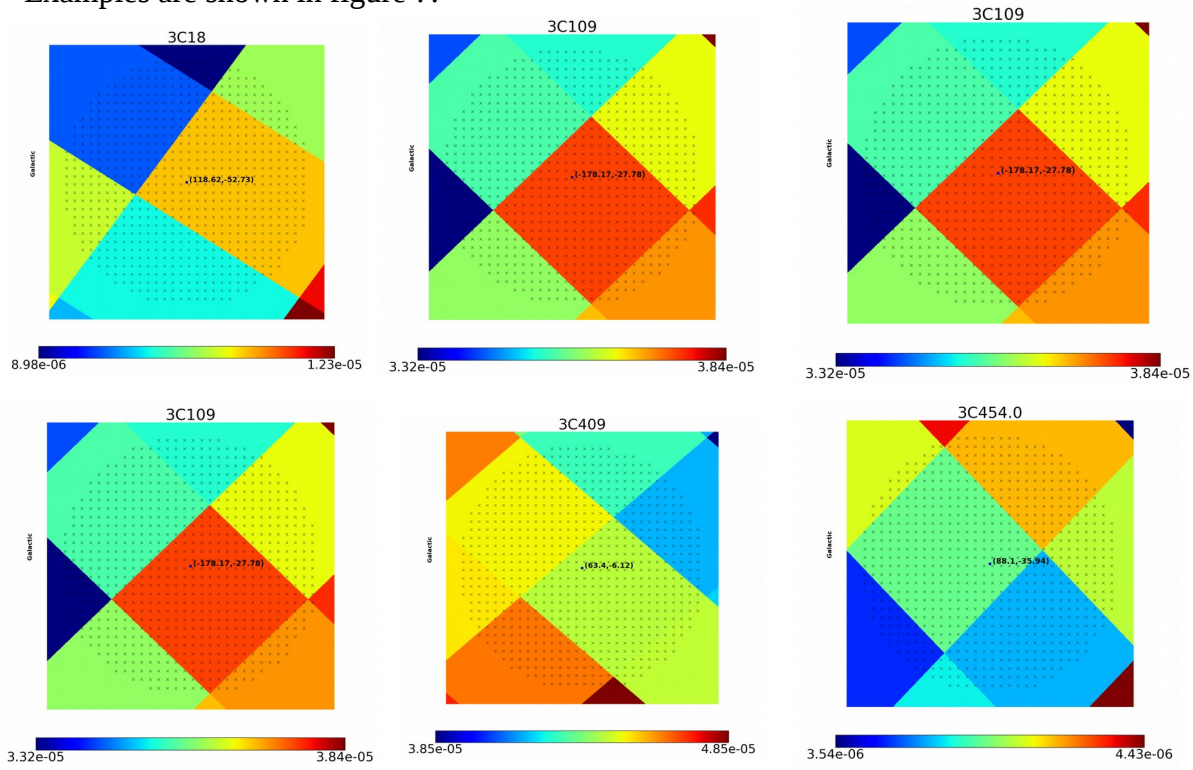

Figure ??: Patches of τ_{353} map around point-sources showing the pixels within the round area of 3.5

arcminutes.

- The errors of the whole τ_{353} map are ~ 5%, see the figure below:

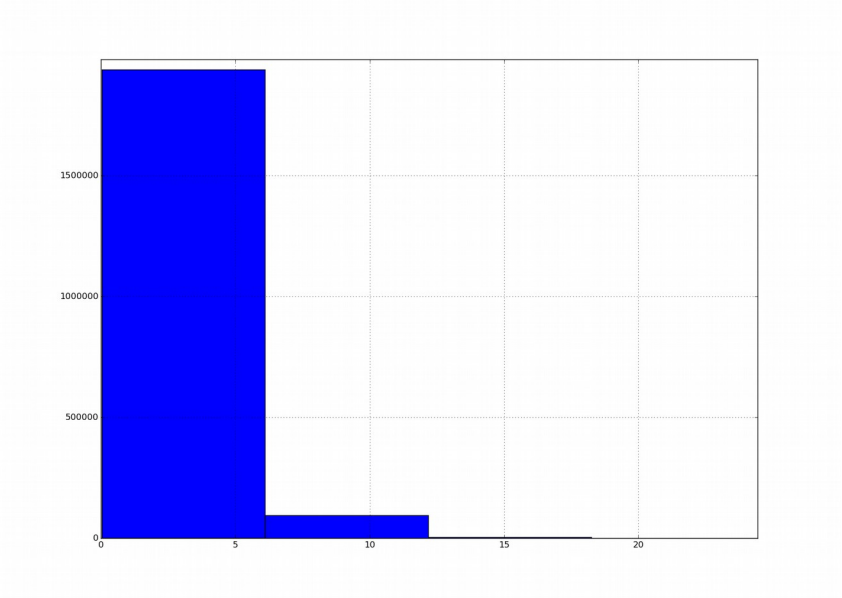

Figure ??: Errors of the τ_{353} map

- Along 26 lines-of-sight without CO, I see that :

+ If use Planck conversion factor, N_H values obtained are closed to Heiles & Troland N_{HI} values (the factor ~ 1.48).

+ If use Fukui conversion factor, N_H values obtained are about double the Heiles & Troland N_{HI} values (the factor ~ 2.31) as shown in below figure.

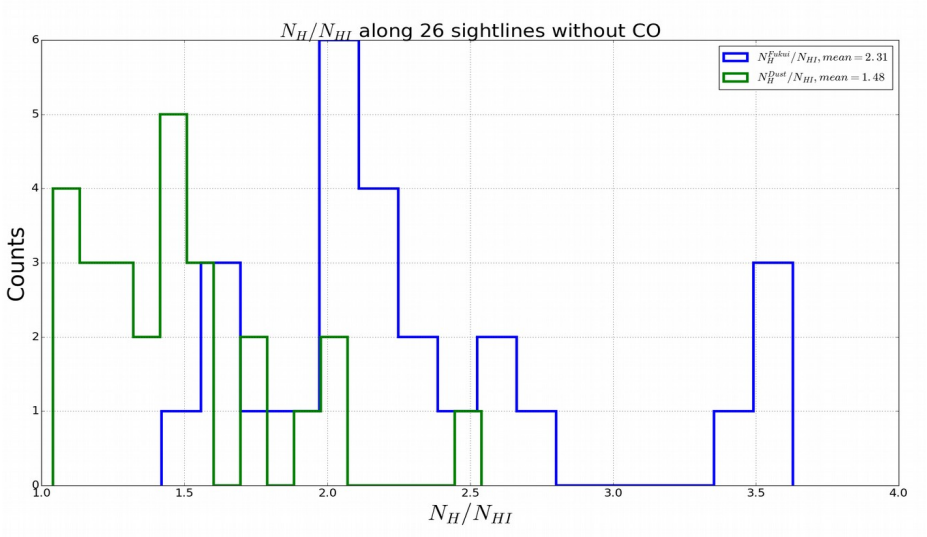

Figure ??: Histogram of N_H/N_{HI} along 26 sources without CO obtained from equations 1 and 2 for Fukui and Planck conversion factors respectively. The mean value of N_{H_Fukui}/N_{HI} = 2.31 and N_{H_Dust}/N_{HI} = 1.48

- Considering only 26 sources without the presence of CO, there is a agreement in Total Gas Column Density values N_H (N_{HI} in fact) obtained from Millennium Survey and Planck data on

thermal dust optical depth τ_{353}. In the assumption of optically thick HI emission line that Fukui et al. 2015 made, the N_H calculated from 26 selected sources using their conversion factor is about twice higher.

- I've just found some interesting information:
1. The distribution of $N_{HI\_Fukui}/N_{HI\_Heiles}$ that I computed is comparable to that from the paper Fuikui et al. 2015, both of them are about 1.0-3.0. Please see the figure below.

(Jo: Hmm... I guess this doesn't seem too surprising, considering that our sub-sample of sight lines in this HI-only analysis tends to be dominated by warm HI (is that right?). i.e. the N(HI)_heiles values are not vastly different from the optically thin HI values? Then the ratio of N(HI_fukui)/N(HI)_thin shouldn't be too different to N(HI_fukui)/N(HI)_heiles.)

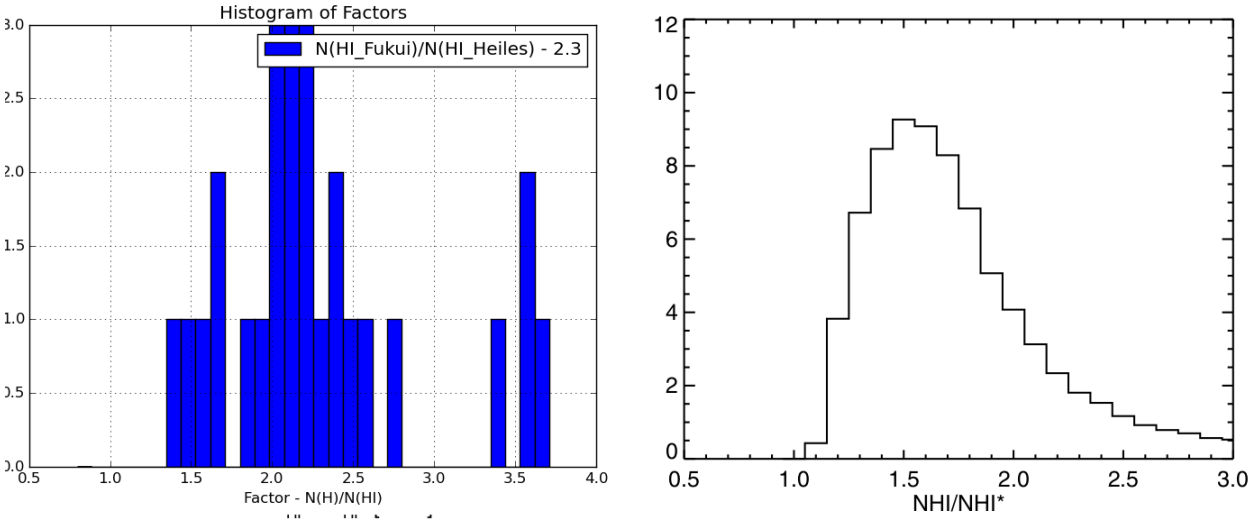

Figure 13. Histograms of (a) $N_{\rm H\,I} - N^*_{\rm H\,I}$ and (b) $N_{\rm H\,I}/N^*_{\rm H\,I}$ shown in Figure 12.

Yes, that's right, the sub-sample (26 sources) is dominated by Warm HI. There are 19/26 light-of-sights having $N_{HI\_Warm} > N_{HI\_Cold}$, and so 7/26 sources with $N_{HI\_Warm} < N_{HI\_Cold}$. *(Please see figure ??)*. In this figure, I just want to check if I'm correct.

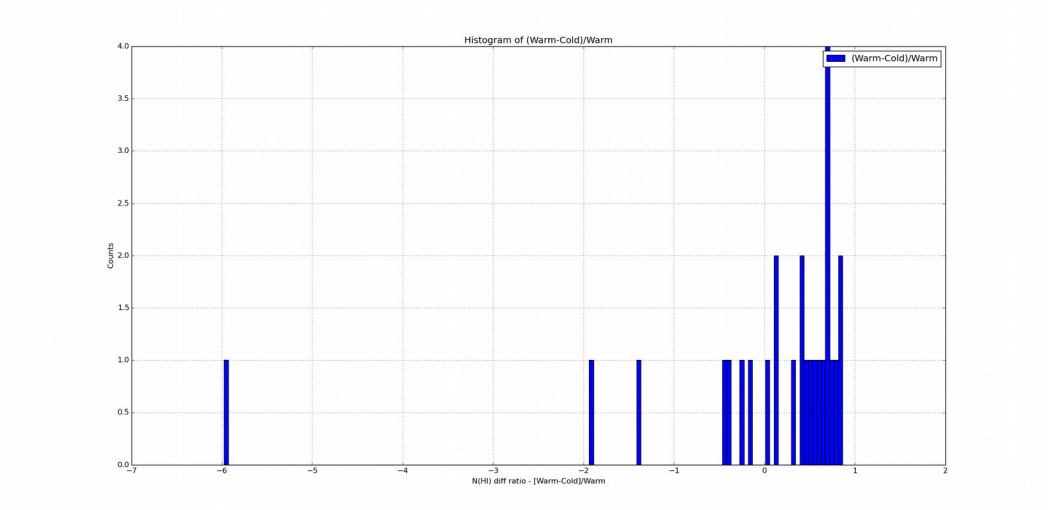

Figure ??: Comparison between N_{CNM} and N_{WNM}.

2. I calculated $f = N_{H\_planck}/N_{HI}$ then I plot: f *vs* N_{HI}. It seems that there is a linear relation between them f and N_{HI} as illustrated in the figures below:

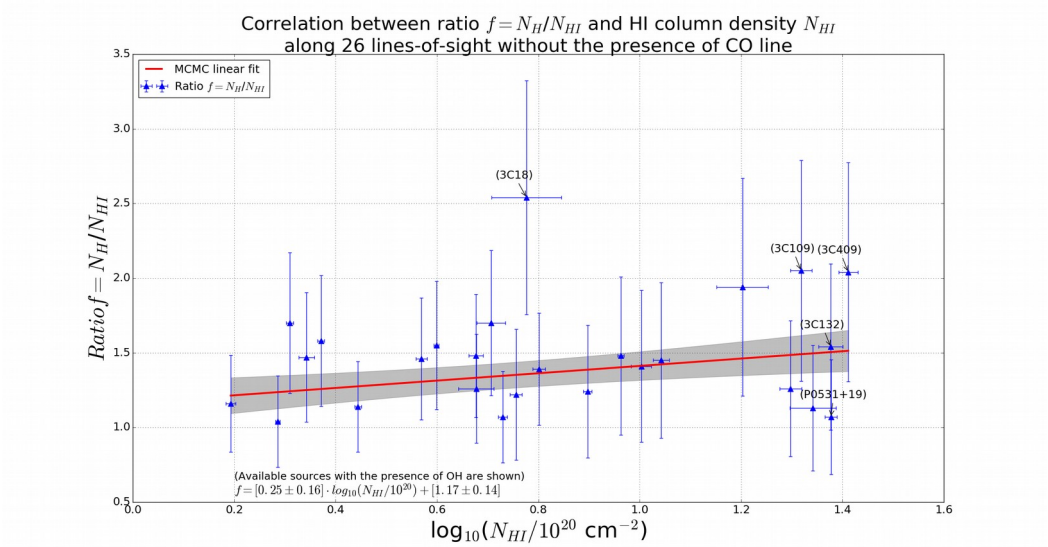

Figure ??: The ratio $f = N_H / N_{HI}$ as a function of $\log_{10}(N_{HI}/10^{20}\ cm^{-2})$. The linear fit determined for 26 data points without the presence of CO is indicated as red line.

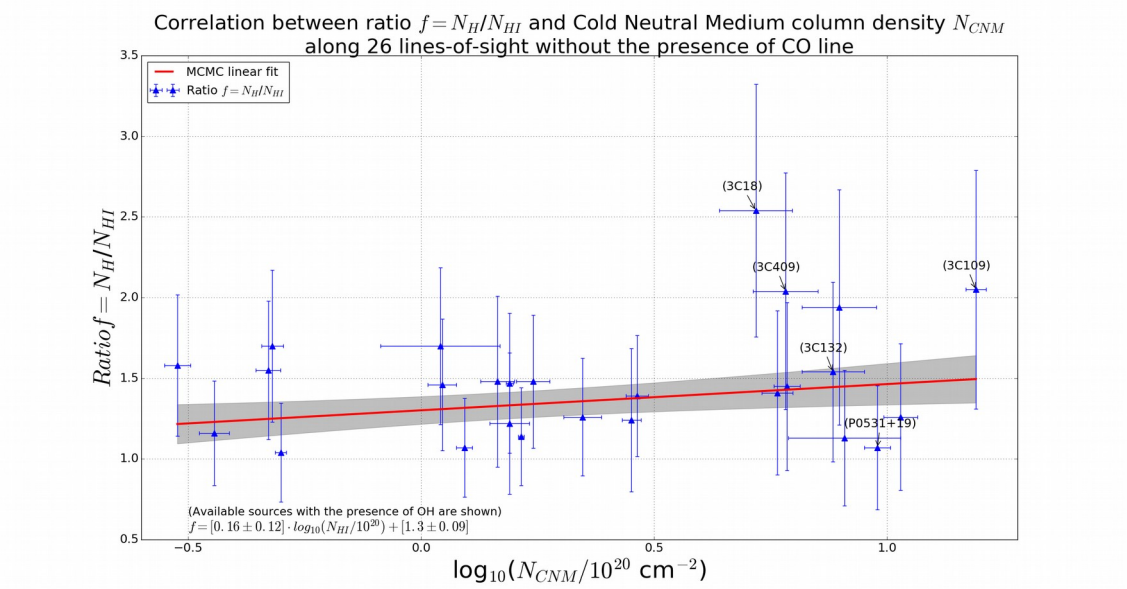

Figure ??: Same as Figure ?? above but only for Cold Neutral Medium. The linear fit is indicated as red line.

(First thoughts: there is more hidden material as you go to higher HI column densities (and the Fukui factor just overestimates things more). If true, this is definitely very interesting! It says there is a larger fraction of dark ISM (presumably CO-dark H2 in our case since Heiles' numbers already include opaque HI) where there is more HI to begin with. What I hope/suspect should be driving this correlation is a correlation between the factor and larger CNM column densities. i.e. you find more CO-dark H2 where the atomic gas tends to be colder/denser. Can you compare that? Plot log(N(HI)_heiles[cold components only]) vs the factor? That plot would be interesting to see!)

- Large fraction of CO-dark H 2 is found in the sightlines where there is more atomic hydrogen. From the correlation between the ratio f and CNM column densities, it seems that one can find more

CO-dark H 2 where the atomic gas tends to be colder or denser.

- I have so far used the offset ~1 beam width (3.5') around the sources, but as illustrated below, I also calculated for larger offsets for comparison, x-axis N_{HI} from Tau_{353} divided by the N_{HI} from Heiles and Troland:

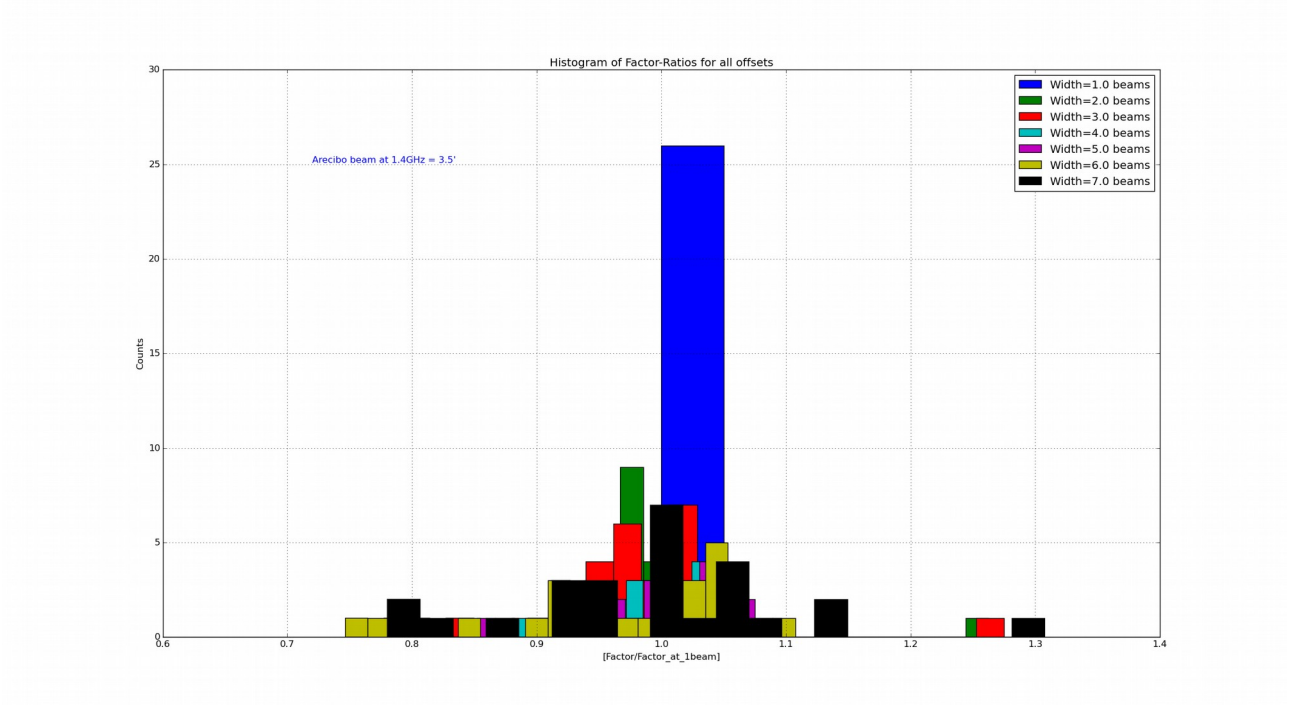

Figure ??:

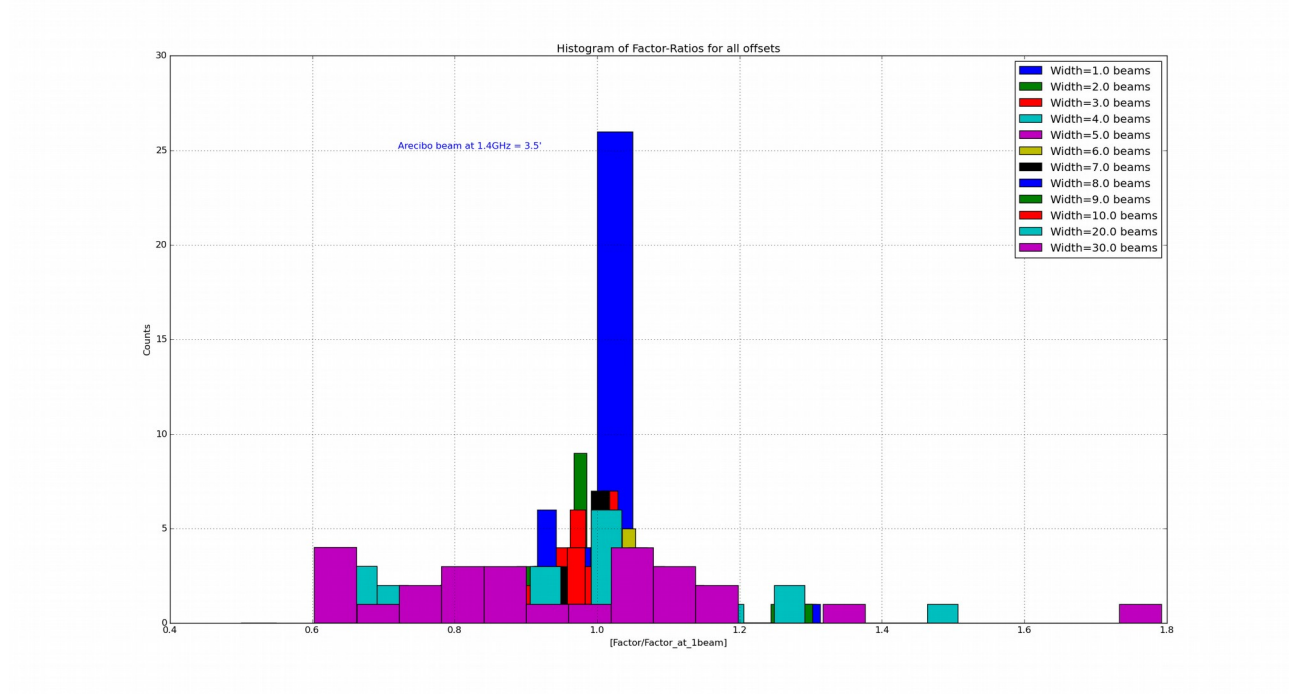

- I see that the ratio of N_{H_Planck} at all offsets is close to it at offset of 1 beam-width.
- The distribution of ratios for all offsets.

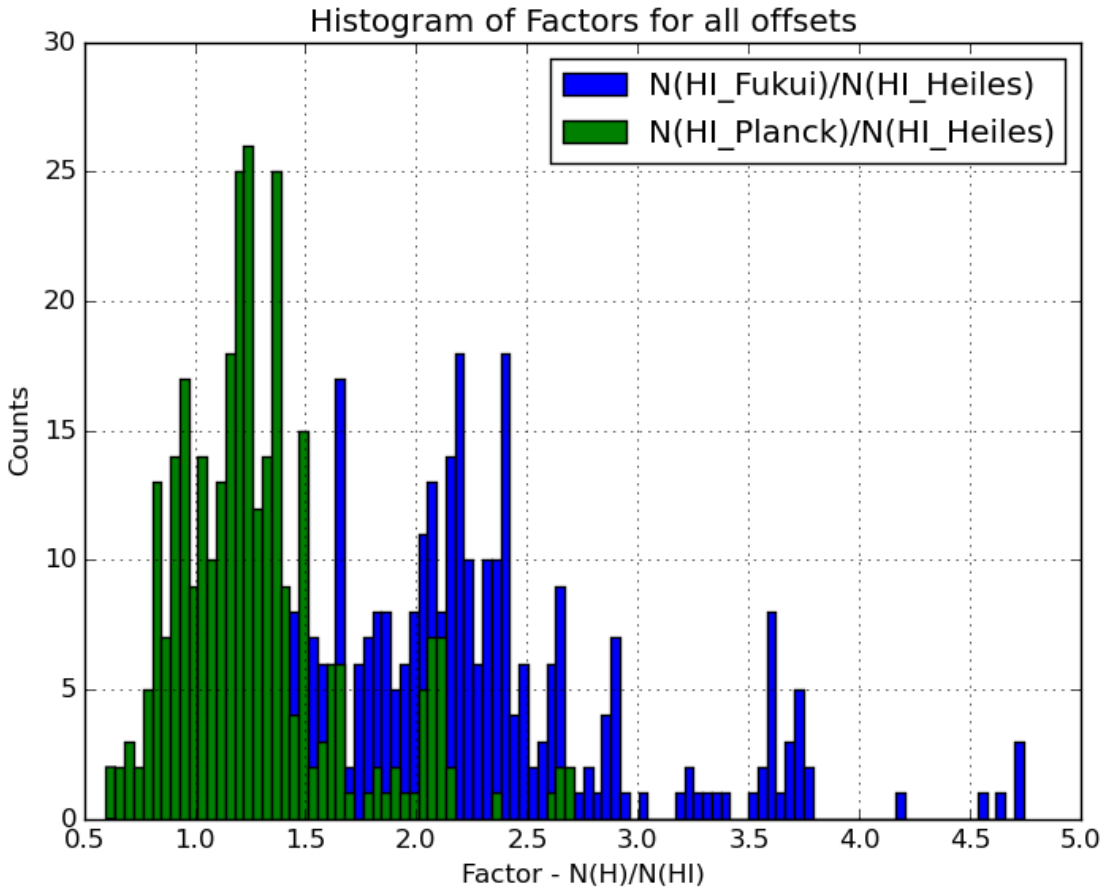
Histogram of Factors for all offsets
N(HI_Fukui)/N(HI_Heiles)
N(HI_Planck)/N(HI_Heiles)
Counts
Factor - N(H)/N(HI)
0
5
10
15
20
25
30
0.5
1.0
1.5
2.0
2.5
3.0
3.5
4.0
4.5
5.0

Figure ??: